AEM
Journals.ASM.org

Anoxygenic Photosynthesis Controls Oxygenic Photosynthesis in a Cyanobacterium from a Sulfidic Spring

Judith M. Klatt,[a] Mohammad A. A. Al-Najjar,[a,b] Pelin Yilmaz,[a] Gaute Lavik,[a] Dirk de Beer,[a] Lubos Polerecky[a,c]

Max Planck Institute for Marine Microbiology, Bremen, Germany[a]; Red Sea Research Center, KAUST, Thuwal, Saudi Arabia[b]; Department of Earth Sciences—Geochemistry, Faculty of Geosciences, Utrecht University, Utrecht, The Netherlands[c]

Before the Earth's complete oxygenation (0.58 to 0.55 billion years [Ga] ago), the photic zone of the Proterozoic oceans was probably redox stratified, with a slightly aerobic, nutrient-limited upper layer above a light-limited layer that tended toward euxinia. In such oceans, cyanobacteria capable of both oxygenic and sulfide-driven anoxygenic photosynthesis played a fundamental role in the global carbon, oxygen, and sulfur cycle. We have isolated a cyanobacterium, *Pseudanabaena* strain FS39, in which this versatility is still conserved, and we show that the transition between the two photosynthetic modes follows a surprisingly simple kinetic regulation controlled by this organism's affinity for H_2S. Specifically, oxygenic photosynthesis is performed in addition to anoxygenic photosynthesis only when H_2S becomes limiting and its concentration decreases below a threshold that increases predictably with the available ambient light. The carbon-based growth rates during oxygenic and anoxygenic photosynthesis were similar. However, *Pseudanabaena* FS39 additionally assimilated NO_3^- during anoxygenic photosynthesis. Thus, the transition between anoxygenic and oxygenic photosynthesis was accompanied by a shift of the C/N ratio of the total bulk biomass. These mechanisms offer new insights into the way in which, despite nutrient limitation in the oxic photic zone in the mid-Proterozoic oceans, versatile cyanobacteria might have promoted oxygenic photosynthesis and total primary productivity, a key step that enabled the complete oxygenation of our planet and the subsequent diversification of life.

Oxygenic photosynthesis (oxygenic P) couples the power of two photosystems (photosystem I [PSI] and PSII) for the extraction of electrons from water (equation 1) to reduce CO_2.

$$2\,H_2O \rightarrow O_2 + 4\;\;H^+ + 4\;\;e^- \qquad (1)$$

Nowadays, this metabolism drives the major part of Earth's ecosystems by providing its products, oxygen and organic carbon, to other organisms. However, oxygenic P has not always been the dominant photosynthetic process. From its evolution, which began possibly more than 3 billion years (Ga) ago (1), until its final success in oxygenating the atmosphere and biosphere (0.58 to 0.55 Ga ago), oxygenic P always had to compete with anoxygenic P, which uses alternative reduced electron donors, such as hydrogen sulfide (equation 2) (2):

$$H_2S \rightarrow S^0 + 2\;\;H^+ + 2\;\;e^- \qquad (2)$$

Intriguingly, cyanobacteria could have made a major contribution to primary productivity by both oxygenic P and anoxygenic P for billions of years (2), and this photosynthetic versatility was probably the key to their success in a reduced world. The balance between oxygenic P and anoxygenic P was probably dependent on environmental conditions, e.g., the light, nutrient, and H_2S gradients. An understanding of how and why the global balance between oxygenic and anoxygenic P has changed on a geological time scale is therefore tightly connected to understanding of (i) the regulation of the switch between the two photosynthetic modes, which is dependent on relevant environmental conditions, and (ii) the C- and N-based growth rates accompanying the respective photosynthetic modes. Such an understanding can be achieved only by studying contemporary model organisms.

It has been known since the 1970s that few extant cyanobacteria are still able to switch between anoxygenic and oxygenic P (3). Such cyanobacteria are presently found exclusively in systems where they are regularly exposed to sulfide, such as phototrophic microbial mats (4). So far, several factors that appear to play a regulatory role in the partitioning between oxygenic and anoxygenic P have been identified: (i) the H_2S concentration, which is connected both to the toxicity of H_2S for photosystem II (5) and to the concentration-dependent activity of sulfide:quinone oxidoreductase (SQR), which drives H_2S oxidation in anoxygenic P (6, 7), (ii) the duration of exposure to sulfide and light, because *de novo* synthesis of SQR has to be induced (8), and (iii) the spectral quality of the light, because anoxygenic P is driven exclusively by PSI, while oxygenic P depends on both PSI and PSII, which have different absorption spectra (9). However, little progress has been made on the details of the regulation of the transition between anoxygenic and oxygenic P in versatile cyanobacteria.

In this study, we investigated how the transition between anoxygenic and oxygenic P is regulated in cyanobacteria that are capable of simultaneous anoxygenic and oxygenic photosynthesis. Specifically, we isolated a monocyanobacterial culture of a *Pseudanabaena* sp. from thin microbial mats forming in a cold sulfidic spring in Frasassi, Italy (10), and quantified its growth rates and

Received 29 October 2014 **Accepted** 2 January 2015

Accepted manuscript posted online 9 January 2015

Citation Klatt JM, Al-Najjar MAA, Yilmaz P, Lavik G, de Beer D, Polerecky L. 2015. Anoxygenic photosynthesis controls oxygenic photosynthesis in a cyanobacterium from a sulfidic spring. Appl Environ Microbiol 81:2025–2031. doi:10.1128/AEM.03579-14.

Editor: J. E. Kostka

Address correspondence to Judith M. Klatt, jklatt@mpi-bremen.de.

Supplemental material for this article may be found at http://dx.doi.org/10.1128/AEM.03579-14.

doi:10.1128/AEM.03579-14

nutrient requirements in the two photosynthetic modes. Our overall aim was to gain insights into the selective advantages that versatile cyanobacteria might have had in a redox-stratified Proterozoic ocean and to identify external parameters that might have promoted the success of oxygenic P.

MATERIALS AND METHODS

Experimental setup. The experimental batch bioreactor without headspace (see Fig. S1 in the supplemental material) was constructed using a 250-ml round-bottom flask with a ring-joint flange (Duran, Germany). It was closed with a custom-made lid through which sensors for real-time monitoring of O_2, pH, and variable fluorescence were inserted. Tightness was achieved by using O-rings and polyurethane-based sealing material (2K-PUR; Kemper System, Germany). The bioreactor was also equipped with two ports for injection, subsampling, and degassing. A cutoff glass syringe (100 ml) was used as an extension of the bioreactor volume to compensate for the injected/subsampled volume. Subsampling therefore did not lead to dilution or any other disturbance of the culture and its activity. Turbulent mixing was achieved by using two magnet-filled glass bars simultaneously. The temperature was kept constant (15°C) by submerging the bioreactor in a flowthrough water bath connected to a large temperature-controlled water reservoir. Illumination was provided by diodes emitting red (λ_{max}, 690 nm) and orange (λ_{max}, 590 nm) light (H2A1 series; Roithner Lasertechnik, Austria) arranged circularly around the transparent water bath and the glass syringe (see Fig. S1). The photon flux in the center of the medium-filled bioreactor was measured with a fiber optic scalar irradiance microprobe (11) connected to a spectrometer (USB4000; Ocean Optics, USA) and calibrated against a scalar irradiance sensor connected to a LI-250A light meter (Li-Cor Biosciences GmbH, Germany). The current through the diodes was adjusted such that the culture was always exposed to a light mixture in which half the intensity consisted of red light and half consisted of orange light. The vertical and horizontal movement of the light sensors during the calibration confirmed that the light was distributed homogeneously in the bioreactor.

Experimental protocol. The filamentous cyanobacterium studied, strain FS39, was isolated and cultivated as described in the supplemental material. When the culture reached the mid-exponential-growth phase (see Fig. S3 in the supplemental material), it was transferred to the bioreactor, and the NO_3^- and HCO_3^- concentrations were readjusted to their initial values (3 mM NO_3^- and 8 mM HCO_3^-). Subsequently, the bioreactor was tightly closed, and the culture was incubated under specific light conditions. For the measurement of anoxygenic P, sulfide was additionally injected to the bioreactor (final concentration, 0.5 to 10 mM). For selected incubations, the PSII inhibitor DCMU [3-(3,4-dichlorophenyl)-1,1-dimethylurea; dissolved in ethanol] was added to a final concentration of 5 μM (12). During all incubations, the O_2 concentrations, pH, and variable fluorescence were monitored every 5 to 60 s using sensors inserted inside the bioreactor, while total sulfide concentrations ($[\sum H_2S] = [H_2S] + [HS^-] + [S^{2-}]$) were analyzed in subsamples collected every 10 to 20 min. During selected incubations, $H^{13}CO_3$ (~10% ^{13}C label) and $^{15}NO_3^-$ (~20% ^{15}N label) were also injected into the bioreactor to enable the quantification of rates of inorganic carbon and nitrate uptake into biomass. Prior to each culture incubation, culture-free medium was incubated for at least 48 h to confirm the tightness of the bioreactor and to determine the rates of oxygen and sulfide removal by abiotic sulfide oxidation.

Analytical procedures. The concentration of dissolved O_2 was measured using an O_2 microelectrode (tip diameter, 100 to 250 μm). The pH was measured with a LIX microsensor (tip diameter, >50 μm) with a double-junction reference electrode (REF251; Radiometer Analytical, France) as well as with a standard laboratory pH probe (InLab Routine-L; Mettler Toledo, Switzerland). Microsensors were built and calibrated as described previously (13, 14).

$[\sum H_2S]$ was determined according to the method of Cline (15). The corresponding concentration of H_2S was then calculated from this $[\sum H_2S]$ according to the work of Millero (16) by using a pK value of 7.14 and the pH measured. Ammonium concentrations in filtered and frozen samples were determined using flow injection analysis (17).

The assimilation of $H^{13}CO_3$ and $^{15}NO_3^-$ into biomass was determined as described previously (18). Subsamples were collected from the reactor and were filtered through a precombusted GF/F filter placed in a syringe filter unit. The filtrate was fixed with $HgCl_2$ and was later used to determine the $^{13}C/^{12}C$ ratio by isotope-ratio-monitoring gas chromatography–mass spectrometry (VG Optima; Micromass, Manchester, United Kingdom) (18). To determine the $^{15}N/^{14}N$ ratio in the filtrate, NO_3^- concentrations just before and directly after the addition of $^{15}NO_3^-$ were quantified using a nitrogen oxide (NOx) analyzer equipped with a chemiluminescence detector (model CLD 66; Eco Physics, Switzerland) (19). The $^{13}C/^{12}C$ and $^{15}N/^{14}N$ ratios in the biomass on the GF/F filters were determined using an automated elemental analyzer (FlashEA, 1112 series) coupled to a Delta Plus Advantage mass spectrometer (Finnigan Delta^{plus}XP) (both from Thermo Scientific) after freeze-drying (18).

Quantification of rates. The rate of oxygenic P (oxyP) and the rate of anoxygenic P (anoxyP) were calculated from the measured concentrations of O_2 and $\sum H_2S$ as $d[O_2]/dt$ and $-d[\sum H_2S]/dt$, respectively. The CO_2 or NO_3^- assimilation rate was calculated as the rate of increase in the isotopic labeling of the biomass corrected for the labeling of the inorganic substrate in the medium (18). All rates were corrected for the growth of the culture by using a growth factor derived from the overall increase in the amount of particulate organic carbon, as determined from mass spectrometry measurements.

RESULTS AND DISCUSSION

***Pseudanabaena* strain FS39.** Phylogenetic analysis revealed that the 16S rRNA sequence of the cyanobacterium studied clustered with those of other *Pseudanabaena* spp. (see Fig. S4 in the supplemental material). Taking its morphology (see Fig. S2 in the supplemental material) into account also, we decided on the name *Pseudanabaena* strain FS39.

Pseudanabaena FS39 is capable of exclusively oxygenic P, simultaneous anoxygenic and oxygenic P, and exclusively anoxygenic P (see below). It can perform anoxygenic P at total sulfide ($\sum H_2S$) concentrations of at least 10 mM. We amplified a *sqr*-like gene (data not shown), which indicated that the initial step of anoxygenic P in this strain, H_2S oxidation, is catalyzed by sulfide: quinone oxidoreductase (SQR), as in *Geitlerinema* sp. PCC 9228 (formerly *Oscillatoria limnetica*), the cyanobacterium that has been most intensively studied for its ability to perform anoxygenic P (7).

Environmental relevance of the induction time for anoxygenic P. In microbial mats, local light, $[H_2S]$, and nutrient availability generally fluctuate dramatically over a diurnal cycle, and cyanobacteria are expected to perform anoxygenic P in the early mornings, when sulfide is abundant in the photic zone (4). In this context, it appears paradoxical that cyanobacteria require an induction time of 2 to 3 h before anoxygenic P starts (8). In *Pseudanabaena* FS39 also, anoxygenic P first had to be induced after cultivation in the absence of sulfide and occurred only after ~2 h of exposure to light and sulfide (Fig. 1). However, if sulfide was injected within 36 h of the subsequent nonsulfidic or dark conditions, anoxygenic P began instantaneously upon exposure to light; that is, the induction lag phase disappeared (Fig. 1). Thus, the induction time is not important in the environment if the organism is exposed to light and sulfide at least once within a diurnal cycle.

Anoxygenic P in *Pseudanabaena* FS39 is controlled by the H_2S concentration and the light intensity. To be able to quantify

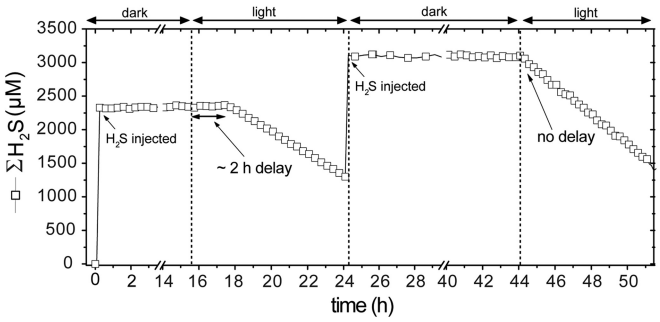

FIG 1 Concentration of total sulfide ($\sum H_2S$) in the bioreactor with *Pseudanabaena* strain FS39 as a function of time. After the initial injection of sulfide, the culture had to be exposed to light for ~2 h for anoxygenic photosynthesis (i.e., $\sum H_2S$ consumption) to start. When the cyanobacteria were left exposed to sulfide in the dark for more than 18 h, no induction time was required, and anoxygenic photosynthesis started immediately after the light was switched on.

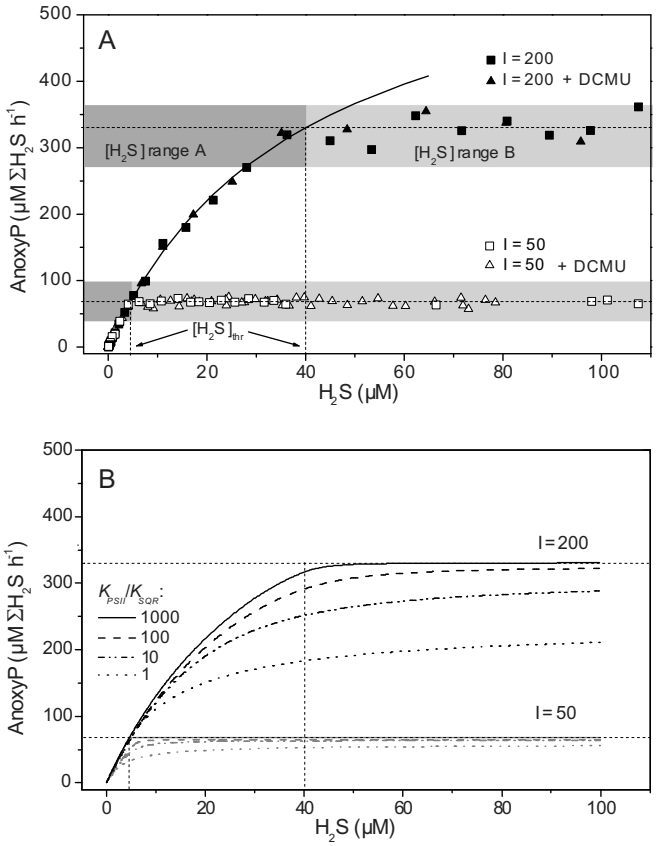

FIG 2 Rate of anoxygenic photosynthesis (anoxyP) as a function of H_2S concentration. (A) Measured rates with illumination at two different light intensities (I), 50 or 200 μmol photons m^{-2} s^{-1}, in the absence or presence of DCMU. Rates below the light-dependent H_2S concentration threshold (i.e., in [H_2S] range A) were fitted with the Michaelis-Menten model for enzyme kinetics by nonlinear regression (thick line) (K_m = 39.1 μM; R^2 = 0.998). Horizontal dashed lines represent $AnoxyP_{max}$ at the indicated light intensity. The corresponding temporal dynamics of $\sum H_2S$ and O_2 are shown in Fig. S7 in the supplemental material. (B) Simulation of anoxygenic photosynthesis in *Pseudanabaena* strain FS39 under the same light conditions, based on the reactions in Fig. 4 and the rate laws in Table 1. The use of different K_{PSII}/K_{SQR} ratios (Table 1) revealed that K_{PSII} has to be at least 2 orders of magnitude greater than K_{SQR} in order to achieve rates of anoxygenic P that are not significantly affected by the rates of oxygenic P.

the rates of exclusively anoxygenic P, we inhibited oxygenic P by using DCMU (see Fig. S7 in the supplemental material). The measurements in this experiment were carried out at two light intensities, 200 and 50 μmol photons m^{-2} s^{-1} (Fig. 2). Unexpectedly, the rates of anoxygenic P (anoxyP) were determined either exclusively by light or exclusively by [H_2S] within the boundaries of two distinct [H_2S] ranges operationally designated A and B (Fig. 2). In concentration range A, i.e., at a low [H_2S], the rates of anoxygenic P followed Michaelis-Menten-like (MM) enzyme kinetics with the sulfide species H_2S (not $\sum H_2S$) as the substrate and were therefore light independent (Fig. 2). Specifically, the apparent affinity constant (K_m) was always 38 μM (±1.2 μM [n = 8]) (Fig. 2 and 3). Upon the transition to [H_2S] range B, anoxyP abruptly stopped increasing and remained constant at a maximum ($AnoxyP_{max}$) (Fig. 2). The threshold [H_2S], above which the transition from range A to range B occurred, as well as the value of $AnoxyP_{max}$, increased with the light intensity.

We propose that in operational [H_2S] range A, anoxyP is determined by the rate of SQR activity (k_{H2S} in Fig. 4). This enzyme catalyzes the oxidation of H_2S to zero-valent sulfur coupled with the reduction of the plastoquinone (PQ) pool. This reaction is light independent (8). The reoxidation of the PQ pool is indirectly governed by light, because light energy harvested in PSI drives overall electron transport. This makes PSI the "bottleneck" of electron transport before the onset of light saturation effects downstream of PSI. We therefore suggest that $AnoxyP_{max}$ reflects the maximum rate of electron flow through PSI (k_{PSI}), which is dictated by the light quanta harvested by this photosystem. Thus, light-independent SQR enzyme kinetics seem to control the rate of anoxygenic P at low [H_2S] (Fig. 2, range A), while light intensity determines the upper limit ($AnoxyP_{max}$) of the process at higher [H_2S] (Fig. 2, range B).

Oxygenic P in *Pseudanabaena* FS39 does not affect anoxygenic P. In the absence of DCMU, we measured simultaneous oxygenic and anoxygenic P. Since oxygenic-P-driven electron transport and anoxygenic-P-driven electron transport intersect in the PQ pool (Fig. 4), we expected that the rates would influence each other by competing for the PQ pool. However, our data showed that the kinetics of anoxygenic P were not significantly affected by oxygenic P, because the $\sum H_2S$ removal rates in the absence and presence of DCMU were indistinguishable (Fig. 2). Therefore, anoxygenic P always occurred at a rate that was determined either by the [H_2S] or by the light intensity. It was not, however, affected by oxygenic P.

Effects of H_2S on oxygenic P. During exclusively oxygenic P, which occurred in the absence of sulfide, the rate of oxygen production at a given light intensity was immediately constant after the light was switched on and remained at this constant level independently of the oxygen concentration in the range of 0 to 900 μM (see Fig. S5 in the supplemental material). As expected, the rate of oxygenic P (oxyP) increased with the light intensity. Saturation was reached at about 550 μmol photons m^{-2} s^{-1}. Above this intensity, oxyP decreased due to light inhibition (see Fig. S6 in the supplemental material).

In the presence of H_2S, a complex relation between anoxyP and oxyP was observed. As described above, anoxyP increased with [H_2S] according to MM kinetics below the light-specific [H_2S] threshold (range A) and then remained constant at a light-depen-

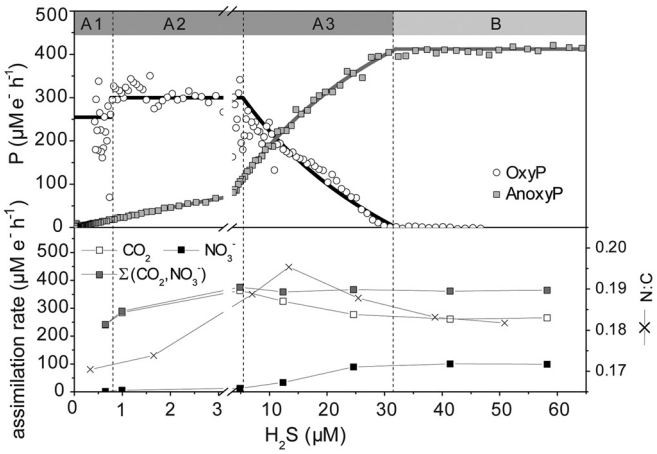

FIG 3 Rate of anoxygenic P (anoxyP) and rate of oxygenic P (oxyP) (top), and nitrate and carbon dioxide assimilation rates and the N/C ratio of the bulk biomass (bottom), as functions of H_2S concentration during exposure to 200 μmol photons m^{-2} s^{-1}. Thick lines represent modeled rates (based on Michaelis-Menten kinetics; K_m = 37.1 μM). Rates were converted to μM e^- h^{-1} as follows: oxyP, expressed in μM O_2 h^{-1}, was multiplied by 4 (equation 1); anoxyP, expressed in μM $\sum H_2S$ h^{-1}, was multiplied by 2 (equation 2); and rates of CO_2 and NO_3^- assimilation were multiplied by 4 and 8, respectively. Annotations above the graphs indicate the operational [H_2S] ranges (A1, A2, A3, B) of the complex switch between the photosynthetic modes. Further examples are shown in section S5 in the supplemental material.

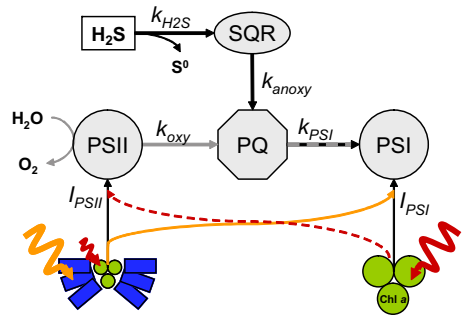

FIG 4 Simplified model of the intersecting oxygenic and anoxygenic photosynthetic electron transport pathways. Chlorophyll *a* (Chl *a*) is the main light-harvesting pigment in photosystem I (PSI). The phycobilisomes (blue) are the main accessory light-harvesting antennae of photosystem II (PSII), which transfer excitation energy into the Chl *a* (red)-containing reaction center. Excitation energy can be redistributed between the photosystems in state 2 as indicated by the orange and red arrows. k_{oxy} is the rate of plastoquinone (PQ) reduction by PSII, i.e., the rate of oxygenic P. k_{anoxy} is the rate of reduction by sulfide:quinone oxidoreductase (SQR), i.e., the rate of anoxygenic P. k_{PSI} is the rate of PQ oxidation by PSI, which corresponds to the overall photosynthetic electron transport rate. k_{H2S} is the rate of H_2S oxidation by SQR; I_{PSI} and I_{PSII} describe the rate of exciton generation by the light energy harvested in PSI and PSII, respectively.

dent value of $AnoxyP_{max}$ (range B) (Fig. 2 and 3). In [H_2S] range B, *Pseudanabaena* FS39 performed exclusively anoxygenic P. To describe the complex relation between anoxyP and oxyP in [H_2S] range A, we further subdivided range A into [H_2S] ranges A1, A2, and A3 (Fig. 3). Also, for a more meaningful comparison between anoxyP and oxyP, we converted the rates of O_2 production and $\sum H_2S$ consumption into electron equivalents (e^-) according to equations 1 and 2 for oxyP and anoxyP, respectively. OxyP was constant ($OxyP_{max1}$) in range A1 (low [H_2S]), increased abruptly from range A1 to A2, and remained constant in range 2 at a higher level ($OxyP_{max2}$) that was, however, still lower than $AnoxyP_{max}$ (Fig. 3). In [H_2S] range A3, oxyP started to decrease. However, the overall sum of photosynthetic electron transport rates and the corresponding CO_2 fixation rates reached their maximum in [H_2S] range A3. In this range, the sum of electron transport by oxygenic and anoxygenic P remained constant at $AnoxyP_{max}$ (413 μM e^- h^{-1}). OxyP could therefore be calculated by subtracting the momentary electron transport rate of anoxyP from the maximum rate observed (oxyP = $AnoxyP_{max}$ − anoxyP) (Fig. 3, thick lines).

Overall, H_2S has two effects on oxyP in *Pseudanabaena* FS39. First, H_2S stimulates oxygenic P ($OxyP_{max2}$ in range A2 [Fig. 3]). Second, H_2S determines anoxyP, which, in turn, defines and limits oxyP (Fig. 3, ranges A3 and B). Thus, anoxyP is regulated exclusively by external factors, namely, the [H_2S] and light intensity, while oxyP is additionally controlled by anoxyP.

Oxygenic photosynthesis is regulated by anoxygenic photosynthesis via the redox state of the PQ pool. The most straightforward explanation of the relation between oxygenic P and anoxygenic P is that the affinity of SQR for PQ is substantially higher than the affinity of PSII components for PQ. We therefore suggest that the mechanistic basis for the outcompetition of oxygenic P by anoxygenic P in *Pseudanabaena* FS39 is simple kinetic regulation. The rate of H_2S oxidation by SQR (k_{H2S}) (Fig. 4) is limiting for anoxygenic P at low [H_2S] (Fig. 2, range A). The rate of PQ reduction by SQR (k_{anoxy}) (Fig. 4) is, however, extremely high. Therefore, oxygenic P is kinetically outcompeted by anoxygenic P. Only if k_{H2S} is lower than the maximum rate of light-specific electron transport through PSI (k_{PSI}) (Fig. 4) will there be sufficient oxidized PQ available to allow oxygenic photosynthetic electron transport (indicated by k_{oxy} in Fig. 4) to occur as well. That is, oxyP fills up the "leftover" electron transport rate. At high [H_2S] (Fig. 2, range B), the rate of electron transport through PSI (k_{PSI}) is limiting. Thus, a light-dependent $AnoxyP_{max}$ is reached, and there is no "leftover" electron transport rate available for oxyP. These kinetic mechanisms imply that the rates of oxygenic P and anoxygenic P are regulated via the redox state of the PQ pool. This is because the rates of reduction (k_{anoxy} and k_{oxy}) and oxidation (k_{PSI}) of the PQ pool depend on its redox state, which, in turn, depends on [H_2S] and light.

We implemented this concept in a numerical model based on Fig. 4 and Table 1 (written in R [www.cran.r-project.org]; for details, see section S6 in the supplemental material), which gave very good agreement with our experimental data (compare Fig. 2A and B). Also, this model revealed that the affinity constant of PSII components for PQ (K_{PSII} in the k_{oxy} equation in Table 1) has to be at least 2 orders of magnitude higher than the affinity constant of SQR (K_{SQR} in the k_{anoxy} equation in Table 1) to fit our experimental data. Also, our model confirmed that the [H_2S] threshold, at which oxygenic and anoxygenic P can occur simultaneously, is predictable for any given light intensity (see section S6.3 in the supplemental material).

Light intensity and H_2S concentration determine the maximal rates of oxygenic photosynthesis. OxyP in the absence of sulfide ($OxyP_{max1}$) was substantially lower than $AnoxyP_{max}$ (Fig. 3). While maximal anoxygenic photosynthetic electron transport depends exclusively on the light energy harvested in PSI, oxygenic photosynthetic electron transport depends on light energy harvested in both PSI and PSII. Since $OxyP_{max1}$ was lower than An-

TABLE 1 Definition of the rate laws governing the reactions shown in Fig. 4

Expression	Description	Explanation of terms
$k_{H2S} = \nu_{\max}\frac{[H_2S]}{K_m + [H_2S]}$	Rate of H_2S oxidation by SQR	K_m (38 ± 1.2 μM) and $\nu_{\max}$ (biomass dependent) were derived by fitting the data below $AnoxyP_{\max}$ in Fig. 2 and 3 and Fig. S8 in the supplemental material.
$k_{anoxy} = k_{H2S}\frac{PQ_{ox}}{K_{SQR} + PQ_{ox}}$	Rate of PQ reduction by SQR	PQ_{ox} refers to the oxidized part of the total PQ pool. K_{SQR} describes the apparent affinity of SQR for oxidized PQ.
$k_{oxy} = I_{PSII}\frac{PQ_{ox}}{K_{PSII} + PQ_{ox}}$	Rate of PQ reduction by PSII	K_{PSII} describes the apparent affinity of PSII for oxidized PQ. I_{PSII} determines the rate of exciton generation by the light energy harvested in PSII, for which we assume a linear relationship to electron transport at a given redox state of the PQ pool for the nonsaturating light intensities used in our experiments. I_{PSII} also defines the maximum rate of oxygenic P, i.e., $OxyP_{\max}$.
$k_{PSI} = I_{PSI}\frac{PQ_{red}}{K_{PSI} + PQ_{red}}$	Total rate of photosynthetic electron transport	K_{PSI} describes the apparent affinity of PSI for reduced PQ. I_{PSI} describes the rate of exciton generation by the light energy harvested in PSI and determines the maximum rate of k_{PSI}, i.e., $AnoxyP_{\max}$. The model assumes that at steady state, k_{PSI} is equal to $k_{oxy} + k_{anoxy}$.

$oxyP_{\max}$, we suggest that oxyP (k_{oxy}) was limited by light energy harvested in PSII. OxyP remained constant at increasing [H_2S] because it was not sufficiently high to fill the "leftover" electron transport rate, and therefore, there was no competition for the PQ pool. This also implies that PSI was substantially more efficient at harvesting light energy than PSII.

Remarkably, $OxyP_{\max1}$ increased abruptly to a higher rate ($OxyP_{\max2}$) when both H_2S and anoxyP reached a threshold. Stimulation of oxygenic P by H_2S has already been reported for plants (20). Those studies, however, involved long-term exposure to H_2S, which leads to a gradual but substantial adjustment of the photosynthetic machinery (such as the activity of RuBisCO [20]). Also, enhancement of CO_2 fixation rates during oxygenic P has been reported for a cyanobacterium (6). The transition between $OxyP_{\max1}$ and $OxyP_{\max2}$ in our study organism, *Pseudanabaena* FS39, occurred within less than 5 min. We therefore suggest that a plausible mechanism behind the increase in oxyP is state transition.

State transitions are commonly used by cyanobacteria to adapt to short-term fluctuations (e.g., in light intensity) so as to adjust the light energy distribution and the resultant electron transport rate between PSI and PSII (21). In state 1, the processes of energy harvesting in PSI and PSII are uncoupled, while excitation energy is transferred from PSII to PSI in state 2 to enhance PSI activity (21). Specifically, in state 1, the phycobilisomes are associated with PSII, whereas in state 2, the excitation energy harvested by the phycobilisomes also drives PSI activity (22). In addition, the energy harvested by chlorophyll *a* (Chl *a*) can be redistributed from PSII to PSI (23).

To explain all our data, we needed to assume that excitation transfer is also possible in the other direction, i.e., from the Chl *a* in PSI to PSII. Although this has never been shown directly, that does not mean that it is theoretically impossible, especially considering how the absorption, excitation, and emission spectra of photosystems I and II can differ among cyanobacterial species and depend on growth conditions (24). Also, bidirectional excitation transfer might not have been demonstrated previously because under "normal conditions," in the absence of H_2S, state transition is induced by a reduced PQ pool, which can be caused only by limited light energy availability in PSI relative to that in PSII. The resulting "electron traffic jam" is removed by transferring more light energy to PSI (21). In contrast, in our experiment, light energy is limiting in PSII. Still, due to the combined activity of SQR (k_{anoxy}) and oxygenic P (k_{oxy}), the PQ pool can become reduced. When the sum of these activities reaches a certain threshold, leading to a highly reduced PQ pool, a state transition might occur.

To test this hypothesis, we performed additional incubations at different spectral qualities of light (targeting either PSI or PSII) (see section S5 in the supplemental material) and implemented bidirectional state transition in our numerical model (see section S6 in the supplemental material). The simulated data agreed with the experimental data remarkably well (compare Fig. S8 and S10 in the supplemental material). Also, in contrast to changes in the pigment equipment of the cells or even in photosystem stoichiometry (the PSII/PSI ratio in the membranes), state transition can occur very fast. Thus, we conclude that state transition is the most probable mechanism controlling the increase in oxygenic P (going from range A1 to range A2 [Fig. 3]) in the presence of H_2S.

CO_2 and NO_3^- assimilation. The electrons derived either from H_2S during anoxygenic P or from H_2O during oxygenic P end up reducing $NADP^+$ to NADPH in the last step of the electron chain. In order to understand the fate of the photosynthetically produced NADPH in *Pseudanabaena* FS39, we converted the rates of CO_2 and NO_3^- assimilation into rates in electron equivalents. Figure 3 shows that the CO_2 assimilation rate per electron extracted during photosynthesis was lower during anoxygenic P than during oxygenic P. Specifically, up to 20% of the electrons available from H_2S oxidation were channeled into NO_3^- reduction at the expense of CO_2 reduction. In contrast, during oxygenic P, as much as 90% of the NADPH potentially reduced during exclusively oxygenic P was channeled into CO_2 reduction. The NO_3^- reduction rates decreased to below the detection limit (Fig. 3), despite the lack of an alternative N source, such as ammonium (data not shown). Based on this change in the CO_2/NO_3^- assimilation ratio, we suggest that during the first step of anoxygenic P, i.e., the oxidation of H_2S to zero-valent sulfur by SQR, protons are not translocated across the membrane (7) and thus do not contribute to the proton motive force and ATP generation. This leads to a higher cellular NADPH/ATP ratio than in oxygenic P and

favors nitrate reduction over CO_2 reduction, because less ATP than NADPH is required (25).

Even though oxygenic P results in higher CO_2 fixation rates per electron transported, growth rates are not necessarily lower during anoxygenic P. This is because the final CO_2 fixation rate is a result of both the electron transport rate (higher during anoxygenic P) and the efficiency of the conversion of reducing power into biomass (higher during oxygenic P). Interestingly, these two factors can compensate for each other, leading to equivalently high CO_2 fixation rates during exclusively anoxygenic and exclusively oxygenic P (Fig. 3). Interestingly, the balance between the electron transport rate and the efficiency of energy conservation (given by ATP generation per electron transported) is optimal only during simultaneous oxygenic and anoxygenic P (Fig. 3, range A3). Also, during this simultaneous anoxygenic and oxygenic P, the N/C uptake ratio is close to the Redfield ratio (Fig. 3).

Implications. We have shown that the regulation of the switch between anoxygenic and oxygenic P in *Pseudanabaena* FS39 is determined predominantly by the rate of anoxygenic P. This is because anoxygenic P kinetically outcompetes oxygenic P in the step that transfers electrons to the PQ pool. This outcompetition of oxygenic P in the electron transport chain, however, does not imply that this process is outcompeted in the cyanobacterium under environmental conditions. Instead, this simple regulatory mechanism allows very rapid and efficient adjustment of photosynthetic activity when environmental conditions change.

In microbial mats, versatile cyanobacteria switch between anoxygenic and oxygenic P over a diurnal cycle, wherein anoxygenic P is expected to occur in the early mornings and evenings, when sulfide is abundant (4). Intriguingly, the local concentration of sulfide is lowered by the activity of the cyanobacteria themselves due to anoxygenic P. Therefore, efficient sulfide removal and the flexible transition from anoxygenic to oxygenic P, as shown here for *Pseudanabaena* FS39, not only are crucial for rapid adaptation to fluctuating light and sulfide concentrations but also help the cyanobacterium switch to simultaneous oxygenic and anoxygenic P, which results in the highest carbon-based growth rates (Fig. 3).

Nowadays, adaptations of cyanobacteria to sulfide play a role only in some specific sulfidic ecosystems, such as the microbial mats in the Frasassi sulfidic springs, the habitat of *Pseudanabaena* FS39. Additionally, these adaptations do not seem to be linked to the phylogeny of cyanobacteria (5). Thus, most extant cyanobacteria are not equipped with the metabolic potential to perform anoxygenic P.

However, oxygenic P probably evolved from anoxygenic forms of P (26) in a reduced environment and had to thrive in partially sulfidic oceans for billions of years. For instance, photosynthetic microbes in the mid- to late-Proterozoic oceans probably lived in a euphotic zone characterized by downward gradients of light and oxygen opposed by upward gradients of sulfide and nutrients, an environment similar to what we find nowadays condensed in microbial mats and biofilms (27, 28). In this scenario, a stratified two-layer system might have become established across the euphotic zone, with the lower, light-limited layer dominated by anoxygenic P and the upper, oxic, nutrient-limited layer dominated by oxygenic P (2). Planktonic counterparts of *Pseudanabaena* FS39 might have been very successful in such oceans. This is because *Pseudanabaena* FS39 is highly adapted to an environment where aerobic conditions coincide with N limitation and sulfidic conditions coincide with N availability (Fig. 3). The preferential N assimilation during anoxygenic P has also been shown in *Geitlerinema* sp. PCC 9228. That cyanobacterium increases its N_2 fixation rates in the presence of sulfide. Cyanobacteria similar to *Pseudanabaena* FS39 or *Geitlerinema* sp. PCC 9228 would have assimilated N (in the form of either NO_3^- or N_2) during anoxygenic P at the oxic-anoxic interface of the photic zone of the Proterozoic oceans. Over a diurnal cycle, this would have caused a downward shift of this interface, leading to sulfide limitation and N limitation in the zone where there was still light. However, this would not have caused limitation by the electron donor (H_2S) in versatile cyanobacteria similar to *Pseudanabaena* FS39, because they can rapidly shift to oxygenic P and thus continue growing at the same rate. Additionally, possible carryover of nutrients (e.g., NO_3^-) taken up preferentially in deeper layers during anoxygenic P could have provided sufficient support for growth in the upper oxic zone while oxygenic P was conducted in the presence of more light. This means that the proliferation of oxygenic P would not have been greatly disadvantaged by nutrient limitation, which might have driven primary productivity in general to higher levels. Thus, the adaptation strategy of cyanobacteria such as *Pseudanabaena* FS39 might represent an important intermediate step in evolution. Not only might such cyanobacteria have set the stage for obligately oxygenic phototrophs by their sulfide removal activity, but their adaptation strategy might also have created sufficient pressure on the obligately oxygenic phototrophs to evolve new strategies to cope with N limitation, such as N_2 fixation in the presence of oxygen, which is thought to represent a key factor that led to the proliferation of oxygenic P and the consequent depletion of sulfide and outcompetition of anoxygenic phototrophs—including *Pseudanabaena* FS39-like organisms.

In general, the ability to perform both oxygenic and anoxygenic P was probably an important trait of cyanobacteria for large intervals of the Earth's history and played a crucial role in shaping primary productivity on a global scale (2). This is echoed in the astonishingly smooth and simple kinetic regulation of the transition between anoxygenic and oxygenic P in *Pseudanabaena* FS39. The simplicity of the regulation is especially remarkable considering how complex the adjustment of photosynthesis to changing environmental parameters can be. For instance, Gan et al. (24) recently reported that a *Leptolyngbya* sp. changes the relative transcript levels for >40% of its genome during photoacclimation to far-red light. In contrast, the simplicity of the control of anoxygenic P in *Pseudanabaena* FS39 suggests that anoxygenic P represents an extremely basic part of photosynthetic metabolism, so important that it even regulates oxygenic P.

ACKNOWLEDGMENTS

We thank the technicians from mechanical and electronic workshops for invaluable help during the construction of the experimental setup, the technicians of the microsensor group for microsensor construction, M. Kuypers and H. Schulz-Vogt for providing access to lab facilities, G. Klockgether for support during mass spectrometry measurements, K. Bischof for providing the diving PAM instrument, M. Kuypers, F. Widdel, U. Fischer, and A. Chennu for inspiring discussions, J. Macalady and D. S. Jones for support during sampling, A. Montanari and P. Metallo for the enjoyable atmosphere at the Osservatorio Geologico di Coldigioco during the sampling campaign, and A. Oren and D. Ionescu for providing the *Oscillatoria limnetica* culture.

This work was financially supported by the Max Planck Society.

REFERENCES

1. **Buick R.** 2008. When did oxygenic photosynthesis evolve? Philos Trans R Soc Lond B Biol Sci **363:**2731–2743. http://dx.doi.org/10.1098/rstb.2008.0041.
2. **Johnston DT, Wolfe-Simon F, Pearson A, Knoll AH.** 2009. Anoxygenic photosynthesis modulated Proterozoic oxygen and sustained Earth's middle age. Proc Natl Acad Sci U S A **106:**16925–16929. http://dx.doi.org/10.1073/pnas.0909248106.
3. **Cohen Y, Jørgensen BB, Padan E, Shilo M.** 1975. Sulphide-dependent anoxygenic photosynthesis in the cyanobacterium *Oscillatoria limnetica*. Nature **257:**489–492. http://dx.doi.org/10.1038/257489a0.
4. **Jørgensen BB, Cohen Y, Revsbech NP.** 1986. Transition from anoxygenic to oxygenic photosynthesis in a *Microcoleus chthonoplastes* cyanobacterial mat. Appl Environ Microbiol **51:**408–417.
5. **Miller SR, Bebout BM.** 2004. Variation in sulfide tolerance of photosystem II in phylogenetically diverse cyanobacteria from sulfidic habitats. Appl Environ Microbiol **70:**736–744. http://dx.doi.org/10.1128/AEM.70.2.736-744.2004.
6. **Cohen Y, Jørgensen BB, Revsbech NP, Poplawski R.** 1986. Adaptation to hydrogen sulfide of oxygenic and anoxygenic photosynthesis among cyanobacteria. Appl Environ Microbiol **51:**398–407.
7. **Griesbeck C, Hauska G, Schütz M.** 2000. Biological sulfide oxidation: sulfide-quinone reductase (SQR), the primary reaction, p 179–203. *In* Pandalai SG (ed), Recent research developments in microbiology, vol. 4. Research Signpost, Trivandrum, India.
8. **Arieli B, Padan E, Shahak Y.** 1991. Sulfide-induced sulfide-quinone reductase activity in thylakoids of *Oscillatoria limnetica*. J Biol Chem **266:**104–111.
9. **Oren A, Padan E, Avron M.** 1977. Quantum yields for oxygenic and anoxygenic photosynthesis in the cyanobacterium *Oscillatoria limnetica*. Proc Natl Acad Sci U S A **74:**2152–2156. http://dx.doi.org/10.1073/pnas.74.5.2152.
10. **Galdenzi S, Cocchioni M, Morichetti L, Amici V, Scuri S.** 2008. Sulfidic ground-water chemistry in the Frasassi caves, Italy. J Cave Karst Stud **70:**94–107.
11. **Lassen C, Ploug H, Jørgensen BB.** 1992. A fibre-optic scalar irradiance microsensor: application for spectral light measurements in sediments. FEMS Microbiol Lett **86:**247–254. http://dx.doi.org/10.1111/j.1574-6968.1992.tb04816.x.
12. **Trebst A.** 1980. Inhibitors in electron flow: tools for the functional and structural localization of carriers and energy conservation sites. Methods Enzymol **69:**675–715. http://dx.doi.org/10.1016/S0076-6879(80)69067-3.
13. **Revsbech NP.** 1989. An oxygen microsensor with a guard cathode. Limnol Oceanogr **34:**474–478. http://dx.doi.org/10.4319/lo.1989.34.2.0474.
14. **De Beer D, Schramm A, Santegoeds CM, Kühl M.** 1997. A nitrite microsensor for profiling environmental biofilms. Appl Environ Microbiol **63:**973–977.
15. **Cline JD.** 1969. Oxygenation of hydrogen sulfide in seawater at constant salinity, temperature and pH. Environ Sci Technol **3:**838–843. http://dx.doi.org/10.1021/es60032a004.
16. **Millero F.** 1986. The thermodynamics and kinetics of the hydrogen sulfide system in natural waters. Mar Chem **18:**121–147. http://dx.doi.org/10.1016/0304-4203(86)90003-4.
17. **Hall POJ, Aller RC.** 1992. Rapid, small-volume, flow injection analysis for $\sum CO_2$ and NH_4^+ in marine and freshwaters. Limnol Oceanogr **37:**1113–1119. http://dx.doi.org/10.4319/lo.1992.37.5.1113.
18. **Sheik AR, Brussaard CPD, Lavik G, Foster RA, Musat N, Adam B, Kuypers MMM.** 2013. Viral infection of *Phaeocystis globosa* impedes release of chitinous star-like structures: quantification using single cell approaches. Environ Microbiol **15:**1441–1451. http://dx.doi.org/10.1111/j.1462-2920.2012.02838.x.
19. **Braman RS, Hendrix SA.** 1989. Nanogram nitrite and nitrate determination in environmental and biological materials by vanadium(III) reduction with chemiluminescence detection. Anal Chem **61:**2715–2718. http://dx.doi.org/10.1021/ac00199a007.
20. **Chen J, Wu F-H, Wang W-H, Zheng C-J, Lin G-H, Dong X-J, He J-X, Pei Z-M, Zheng H-L.** 2011. Hydrogen sulphide enhances photosynthesis through promoting chloroplast biogenesis, photosynthetic enzyme expression, and thiol redox modification in *Spinacia oleracea* seedlings. J Exp Bot **62:**4481–4493. http://dx.doi.org/10.1093/jxb/err145.
21. **Allen JF, Mullineaux CW, Sanders CE, Melis A.** 1989. State transitions, photosystem stoichiometry adjustment and non-photochemical quenching in cyanobacterial cells acclimated to light absorbed by photosystem I or photosystem II. Photosynth Res **22:**157–166. http://dx.doi.org/10.1007/BF00035446.
22. **Xu X, Yang S, Xie J, Zhao J.** 2012. Kinetics and dynamics for light state transition in cyanobacterium *Spirulina platensis* cells. Biochem Biophys Res Commun **422:**233–237. http://dx.doi.org/10.1016/j.bbrc.2012.04.131.
23. **McConnell MD, Koop R, Vasil'ev S, Bruce D.** 2002. Regulation of the distribution of chlorophyll and phycobilin-absorbed excitation energy in cyanobacteria. A structure-based model for the light state transition. Plant Physiol **130:**1201–1212. http://dx.doi.org/10.1104/pp.009845.
24. **Gan F, Zhang S, Rockwell NC, Martin SS, Lagarias JC, Bryant DA.** 2014. Extensive remodeling of a cyanobacterial photosynthetic apparatus in far-red light. Science **345:**1312–1317. http://dx.doi.org/10.1126/science.1256963.
25. **Noctor G, Foyer CH.** 1998. A re-evaluation of the ATP:NADPH budget during C_3 photosynthesis: a contribution from nitrate assimilation and its associated respiratory activity? J Exp Bot **49:**1895–1908. http://dx.doi.org/10.1093/jxb/49.329.1895.
26. **Blankenship RE, Sadekar S, Raymond J.** 2007. The evolutionary transition from anoxygenic to oxygenic photosynthesis, p 22–33. *In* Falkowski PG, Knoll, AH (ed), Evolution of primary producers in the sea. Elsevier Academic Press, Amsterdam, The Netherlands.
27. **Canfield DE.** 1998. A new model for Proterozoic ocean chemistry. Nature **396:**450–453. http://dx.doi.org/10.1038/24839.
28. **Fennel K, Follows M, Falkowski PG.** 2005. The co-evolution of the nitrogen, carbon and oxygen cycles in the Proterozoic ocean. Am J Sci **305:**526–545. http://dx.doi.org/10.2475/ajs.305.6-8.526.